

Thermal behaviour and spectroscopic investigation of some methyl 2-pyridyl ketone complexes

Mariana Tătucu · Petre Rotaru · Ileana Rău ·
Cezar Spînu · Angela Kriza

Received: 24 April 2009 / Accepted: 26 June 2009 / Published online: 28 August 2009
© Akadémiai Kiadó, Budapest, Hungary 2009

Abstract Pyridine derivative complexes are widely employed as biological active materials especially as antibacterial agents. Five transition metal(II) mpk complexes (mpk = methyl 2-pyridyl ketone) were synthesized and investigated using elemental analysis, spectroscopic techniques (IR and UV–Vis–NIR) and conductometric measurements. The general formulae established from experimental data were found to be $[M(\text{mpk})_2(\text{NO}_3)_2] \cdot x\text{H}_2\text{O}$ ($x = 0$ for $M = \text{Cd}(\text{II}), \text{Zn}(\text{II}), x = 2$ for $M = \text{Cu}(\text{II})$) and $[M(\text{mpk})_2(\text{H}_2\text{O})_2](\text{NO}_3)_2$ ($M = \text{Co}(\text{II}), \text{Ni}(\text{II})$). These compositions were further confirmed by thermal analysis and their thermal stability in dynamic air atmosphere investigated.

Keywords Methyl 2-pyridyl ketone ·
Transition metal(II) complexes · Thermal analysis

Introduction

Many pyridine derivatives have a great diversity of effects on micro and macroorganisms of both plants and animals which have been attributed to their ability to form complexes with transition or non-transition metals [1–4]. For this reason, we have been interested in the study of transition metal(II) complexes of 2-pyridyl ketones with different anions in solution [5–7]. A weak antimicrobial activity for our methyl 2-pyridyl ketone complexes was observed, and a moderate one for phenyl-2-pyridyl ketone complexes [7].

On the other hand, pyridine derivative complexes show specific characteristics, like the formation of clusters or coordination polymers with interesting magnetic properties [8–10]. A literature survey indicates a high number of publications, to mention some early papers [11, 12], but also new papers as well [13, 14] on the thermal analysis of pyridine–metal complexes. However, regarding the thermal behavior of this kind of complexes there are a rather few information [15, 16].

Usually, most of the coordination compounds are used as biological active materials [17–21] or as source for simple inorganic materials obtaining. Therefore, thermal analysis is an important tool in their characterization and respectively as method for the controlled step-wise obtaining of basic functional materials such as CdS, ZnO, etc. [22–27]. We report here on the thermal behavior and spectroscopic characterization of some transition metal(II) complexes with methyl 2-pyridyl ketone (mpk) (Fig. 1).

M. Tătucu
Faculty of Pharmacy, University of Medicine and Pharmacy
of Craiova, 1 May Avenue, Nr. 66, Craiova, Romania

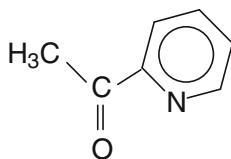
P. Rotaru (✉)
Faculty of Physics, University of Craiova, A.I. Cuza Str., Nr. 13,
Craiova, Romania
e-mail: protaru@central.ucv.ro; petrerotaru@yahoo.com

I. Rău
Faculty of Applied Chemistry and Materials Science, University
“Politehnica” Bucharest, Polizu Str., Nr. 1, Bucharest, Romania

C. Spînu
Faculty of Chemistry, University of Craiova,
Calea Bucuresti Str., Nr. 107 I, Craiova, Romania

A. Kriza
Department of Inorganic Chemistry, Faculty of Chemistry,
University of Bucharest, Dumbrava Rosie Str., Bucharest,
Romania

Fig. 1 Methyl 2-pyridyl ketone (mpk)



Experimental

Samples preparation

The five complex compounds were obtained through synthesis at room temperature and under no agitation. All reagents used in the present study ($\text{Cu}(\text{NO}_3)_2 \cdot 3\text{H}_2\text{O}$, $\text{Co}(\text{NO}_3)_2 \cdot 6\text{H}_2\text{O}$, $\text{Ni}(\text{NO}_3)_2 \cdot 6\text{H}_2\text{O}$, $\text{Zn}(\text{NO}_3)_2 \cdot 6\text{H}_2\text{O}$, $\text{Cd}(\text{NO}_3)_2 \cdot 4\text{H}_2\text{O}$ and mpk) were purchased from Merck and used as received. The synthetic procedure was similar for all complexes: to ethanolic solution (15 cm^3) of methyl 2-pyridyl ketone ($2 \times 10^{-3} \text{ mol} \cdot \text{dm}^{-3}$) was added an ethanol solution (15 cm^3) containing $\text{M}(\text{NO}_3)_2 \cdot x\text{H}_2\text{O}$ ($1 \times 10^{-3} \text{ mol} \cdot \text{dm}^{-3}$). The slow evaporation of the resulting mixtures leads to crystalline powders for Cu(II), Ni(II) and Zn(II) complexes and single crystals for Co(II) and Cd(II) complexes [6].

Techniques

C, H and N elemental analyses were performed on a ECS 4010 elemental analyzer (from Costech Analytical Technologies). FT-IR spectra were recorded as KBr pellets with a FTS 135 spectrometer (from BioRad Corporation) in the $4000\text{--}400 \text{ cm}^{-1}$ range. UV-Vis-NIR spectra were recorded on a V-670 spectrophotometer from Jasco, in reflection-diffusion mode, using MgO as a standard. The magnetic measurements were performed at room temperature using the Faraday method. The conductometric measurements were performed at a Consort C-533 conductometer (from Cole-Parmer) using ethanol solutions ($10^{-3} \text{ mol dm}^{-3}$) at room temperature also.

Thermal analysis measurements (TG, DTG and DSC) of transition metal(II) mpk complexes were carried out in dynamic air atmosphere ($150 \text{ cm}^3 \text{ min}^{-1}$), under non-isothermal linear regimes. A horizontal “Diamond” Differential/Thermogravimetric Analyzer from PerkinElmer Instruments was used during the measurements. Samples from 0.5 to 1.4 mg contained in aluminum crucibles were heated in the temperature range of $20\text{--}600 \text{ }^\circ\text{C}$, each time with the heating rate of 10 K min^{-1} .

Results and discussion

The synthesized complexes are soluble in water, methanol, ethanol, DMF, acetone and chloroform, but insoluble in

carbon tetrachloride and ethyl ether. From elemental analysis data (Table 1) an 1:2 metal:ligand stoichiometry was determined. Molar conductance measurements (Table 1) show that new compounds are non-electrolytes, except for those containing cobalt(II) and nickel(II), which are electrolytes of the type 1:2. Based on these observations, the chemical formulae attributed to new compounds are $[\text{M}(\text{mpk})_2(\text{NO}_3)_2] \cdot x\text{H}_2\text{O}$ ($x = 0$ for $\text{M} = \text{Cd}(\text{II}), \text{Zn}(\text{II})$, $x = 2$ for $\text{M} = \text{Cu}(\text{II})$) and $[\text{M}(\text{mpk})_2(\text{H}_2\text{O})_2](\text{NO}_3)_2$ ($\text{M} = \text{Co}(\text{II}), \text{Ni}(\text{II})$).

IR spectroscopy

In order to determine the coordination mode of the mpk ligand, IR transmission spectra were recorded ($4000\text{--}400 \text{ cm}^{-1}$) for both free ligand and for each new complex combination (Table 2).

As can be seen in Table 2, the IR spectrum of the ligand shows a vibration band at 1723 cm^{-1} , which is specific to the stretching vibration of the carbonyl group [28]. The same vibration band appears shifted with $\sim 40\text{--}100 \text{ cm}^{-1}$ toward lower wavenumbers for the complex 1–5. This suggests that the ligand coordinates to the metal ions through the oxygen atom of the carbonyl group.

Moreover, the vibration band which appears in the IR spectrum of the ligand at 1585 cm^{-1} and corresponds to the stretching vibration of the pyridine group ($\text{C}=\text{N}$) [28], appears also in the IR spectra of the complexes at higher wavenumber ($7\text{--}25 \text{ cm}^{-1}$ higher), proving the coordination of the nitrogen atom from the pyridine ring to the metal center.

All compounds (except for 5) exhibit a broad and relatively intense band at $3400\text{--}3200 \text{ cm}^{-1}$ which indicates the presence of water molecules. This band corresponds to the (O–H) stretching vibration. For 2 and 3, this band is accompanied by two bands in the $900\text{--}700 \text{ cm}^{-1}$ range, assigned to the rocking and wagging modes of (O–H) group [28]. This suggests that the water molecules are indeed coordinated. This fact is also sustained by the X-ray diffraction studies [6] for cobalt(II) compound. In the IR spectra of 1 and 4 the latter bands are not observed confirming that 1 and 4 may rather contain crystallization water.

Two strong vibrations at $1490\text{--}1445 \text{ cm}^{-1}$ and $1300\text{--}1280 \text{ cm}^{-1}$ region, attributed to ν_4 and ν_1 vibration modes of the covalently bonded nitrate groups [16] are also observed. The magnitude of splitting ($\nu_4 - \nu_1$) for the complexes studied herein is about $160\text{--}190 \text{ cm}^{-1}$ suggesting medium-strong covalency for the metal–nitrate bond [29]. It is difficult to establish the nature of coordinated nitrate by infrared studies. However, according to Lever et al. [30] the number and energies of nitrate combination frequencies in the $1800\text{--}1700 \text{ cm}^{-1}$ region of the

Table 1 Elemental analysis and physico-chemical properties of the complexes **1–5**

No.	Compound	%C exp. (calc.)	%H exp. (calc.)	%N exp. (calc.)	Color/look	Λ^a ($\Omega^{-1} \text{ cm}^2 \text{ mol}^{-1}$)
1	[Cu(mpk) ₂ (NO ₃) ₂ ·2H ₂ O	35.99 (36.05)	3.91 (3.86)	11.51 (12.01)	Violet red/crystalline powder	23
2	[Co(mpk) ₂ (H ₂ O) ₂](NO ₃) ₂	36.99 (36.44)	4.01 (3.90)	11.98 (12.14)	Red/single crystals	47
3	[Ni(mpk) ₂ (H ₂ O) ₂](NO ₃) ₂	36.80 (36.44)	4.25 (3.90)	11.73 (12.14)	Green/crystalline powder	49
4	[Zn(mpk) ₂ (NO ₃) ₂]	37.90 (38.97)	4.16 (3.24)	12.13 (12.99)	Colorless/crystals	25
5	[Cd(mpk) ₂ (NO ₃) ₂]	35.89 (35.14)	3.01 (2.92)	11.12 (11.71)	Colorless/single crystals	30

^a Ethanol solutions, $10^{-3} \text{ mol L}^{-1}$ at 20 °C

Table 2 Characteristic infrared absorption frequencies (cm^{-1}) of mpk and **1–5** complexes

No.	Compound	ν (O–H)	$(\nu_4 + \nu_1)$ (NO ₃) [−] coord	$\nu(\text{C}=\text{O})$	$\nu(\text{C}=\text{N})$ Py	$\nu_4(\text{NO}_3)^-$ coord	$\nu(\text{NO}_3)^-$ free	$\nu_1(\text{NO}_3)^-$ coord	δ_r (O–H)	δ_w (O–H)
	mpk (L)	–	–	1723	1585				–	–
1	[Cu(mpk) ₂ (NO ₃) ₂ ·2H ₂ O	3413	1767 1745	1682	1610	1492	–	1306	–	–
2	[Co(mpk) ₂ (H ₂ O) ₂](NO ₃) ₂	3216		1660	1600	–	1384	–	970	781
3	[Ni(mpk) ₂ (H ₂ O) ₂](NO ₃) ₂	3225		1656	1598	–	1384	–	973	792
4	[Zn(mpk) ₂ (NO ₃) ₂]	3416	1772 1747 1731	1629	1603	1470	–	1291	–	–
5	[Cd(mpk) ₂ (NO ₃) ₂]	–	1765 1729	1678	1592	1445	–	1283	–	–

infrared spectra, may be used as an empirical indicator of nitrate coordination modes. Thus, a separation between combination frequencies of $\sim 5\text{--}26 \text{ cm}^{-1}$ indicates a monodentate coordination of nitrate, whereas a difference of $\sim 25\text{--}66 \text{ cm}^{-1}$ suggests a bidentate nitrate [30]. The occurrence of two or three weak bands in the combination bands region of spectra of copper(II) and zinc(II) complexes, suggests a monodentate behavior of nitrate groups.

Infrared spectrum of cadmium(II) complex contains two weak absorptions located at 1765 and 1729 cm^{-1} respectively, which means according to Lever et al. [30] that nitrate groups from this complex are bidentate. The bidentate character of nitrate groups from [Cd(mpk)₂(NO₃)₂] complex has been established previously by X-ray diffraction studies [6].

The infrared spectra of cobalt(II) and nickel(II) complexes show specific bands of free nitrate at 1384 cm^{-1} [28].

Additionally, all spectra of **1–5** exhibit one or two bands which are not found in the free ligand spectrum. These bands appear at lower frequencies, in the 400–500 cm^{-1} range, have medium intensity and correspond to the stretching vibration of the new M–N and M–O bonds [31].

In summary, the infrared spectral data suggest that the mpk ligand acts as bidentate ligand coordinating through

pyridine nitrogen and carbonyl oxygen. The coordination sphere of the metal is completed by the nitrate anions in the case of copper, zinc and cadmium complexes, and by the water molecules for cobalt and nickel complexes.

UV–Vis–NIR spectroscopy

In order to obtain information referring to the geometry of these compounds, the UV–Vis–NIR spectra were registered at room temperature in the 50,000–5500 cm^{-1} range and the data obtained were correlated with magnetic moment values (Table 3) and ligand field parameters 10Dq, B and β .

The UV spectrum of the free ligand displays two absorption bands at 44,050 cm^{-1} and 37,450 cm^{-1} which have been assigned to the $\pi \rightarrow \pi^*$ and $n \rightarrow \pi^*$ transitions, respectively. These transitions have been found also in the spectra of the complexes but shifted to lower wavenumbers ($\Delta\nu = 6000\text{--}8000 \text{ cm}^{-1}$) confirming the coordination of the ligand.

The electronic spectrum of copper(II) complex displays two $d \rightarrow d$ bands with maxima centered at $\sim 17,640$ and $14,290 \text{ cm}^{-1}$ respectively. These spectral features are similar to those reported for the copper (II) ions in a tetragonal distorted octahedral ligand field [32]. For octahedral species of d^9 ions the value of 10Dq parameter is

Table 3 Electronic spectra, magnetic moments and ligand field parameters for mpk and complexes **1–5**

No.	Compound	Absorption maxima (cm ⁻¹)	Assignments	μ_{eff} (B.M.)	Dq (cm ⁻¹)	B (cm ⁻¹)	β
	mpk (L)	44,050	$\pi \rightarrow \pi^*$	–	–	–	–
		37,450	$n \rightarrow \pi^*$				
1	[Cu(mpk) ₂ (NO ₃) ₂] \cdot 2H ₂ O	17,640 (ν_3)	$d_{xz,yz} \rightarrow d_{x^2-y^2}$	1.84	1600	–	–
		14,290 (ν_2)	$d_{xy} \rightarrow d_{x^2-y^2}$				
2	[Co(mpk) ₂ (H ₂ O) ₂](NO ₃) ₂	36,230	$\pi \rightarrow \pi^*$	4.29	1145	885	0.911
		28,735	$n \rightarrow \pi^*$				
		22,125 (ν_3)	${}^4T_{1g}(F) \rightarrow {}^4T_{1g}(P)$				
		10,150 (ν_1)	${}^4T_{1g}(F) \rightarrow {}^4T_{2g}$				
3	[Ni(mpk) ₂ (H ₂ O) ₂](NO ₃) ₂	37,735	$\pi \rightarrow \pi^*$	2.97	1072	646	0.627
		29,585	$n \rightarrow \pi^*$				
		16,340 (ν_2)	${}^3A_{2g}(F) \rightarrow {}^3T_{1g}(F)$				
		10,720 (ν_1)	${}^3A_{2g}(F) \rightarrow {}^3T_{2g}(F)$				
4	[Zn(mpk) ₂ (NO ₃) ₂]	16,800	CT	–	–	–	–
5	[Cd(mpk) ₂ (NO ₃) ₂]	18,180	CT	–	–	–	–

equal with energy of band observed in visible region of the spectrum [32]. The absorption maxima, their assignments, the calculated ligand field parameters and the magnetic moment are presented in Table 3.

The reflectance spectrum of [Co(mpk)₂(H₂O)₂](NO₃)₂ consist of two bands located at 22,125 and 10,150 cm⁻¹ which correspond to $d \rightarrow d$ transitions ${}^4T_{1g}(F) \rightarrow {}^4T_{1g}(P)$ (ν_3) and ${}^4T_{1g}(F) \rightarrow {}^4T_{2g}$ (ν_1) respectively [32]. The spectrum clearly indicates the octahedral geometry of Co(II) complex. This geometry was confirmed by X-ray diffraction measurements [6]. The calculated values of Dq, B and β reasonably agree with those available experimentally for octahedral Co(II) complexes [33].

UV–Vis–NIR spectrum of nickel(II) complex shows two bands at 16,340 and 10,720 cm⁻¹ which are commonly assigned to ${}^3A_{2g}(F) \rightarrow {}^3T_{1g}(F)$ (ν_2) and ${}^3A_{2g}(F) \rightarrow {}^3T_{2g}(F)$ (ν_1) $d \rightarrow d$ transitions of a six-coordinated Ni(II) ion (Table 3) [32]. For d^8 ions in an octahedral environment, the energy of ν_1 corresponds to 10Dq and the value of Dq is obtained from it [33]. The values of Dq, B and β are in good agreement with those expected for Ni(II) compounds in an octahedral geometry [33].

The electronic spectra of [Zn(mpk)₂(NO₃)₂] and [Cd(mpk)₂(NO₃)₂] do not display $d \rightarrow d$ transitions but can be seen one absorption band for each complex in the region 16,000–18,000 cm⁻¹, which may be assigned to a ligand \rightarrow metal charge transfer L \rightarrow M. Both combinations are diamagnetic. The conductometric measurements show that Zn(II) and Cd(II) complexes are non-electrolytes. Considering these results and infrared data we can conclude that zinc and cadmium complexes are characterized by an octahedral geometry and a dodecahedral one, respectively. The geometry for last compound was confirmed by X-ray diffraction measurements [6].

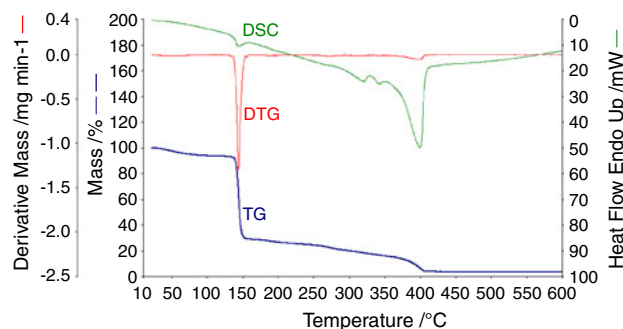
Thermal analysis

Figures 2, 3, 4, 5, and 6 present the thermal analysis curves of the investigated compounds **1–5**. The results concerning thermal decomposition of the five complexes are presented as follows.

Thermal analysis of [Cu(mpk)₂(NO₃)₂] \cdot 2H₂O

For [Cu(mpk)₂(NO₃)₂] \cdot 2H₂O, the thermoanalytical curves (Fig. 2) reveal three well-defined steps of thermal decomposition. A sample of 1.202 mg was used for analysis. The observed mass variation ($\Delta m_{\text{exp}} = 6.77\%$) during the first step corresponds to the loss of two water moles ($\Delta m_{\text{theor}} = 7.70\%$). The low temperature of dehydration (25–80 °C) is an indicative of their nature, namely, crystallization water.

The second stage of decomposition occurring between 140 and 160 °C (experimental mass loss 64.40%) might be interpreted as the loss of both nitrates and one mpk ligand. At this point, exothermic effect (Table 4) very good

**Fig. 2** Thermoanalytical curves of [Cu(mpk)₂(NO₃)₂] \cdot 2H₂O (**1**)

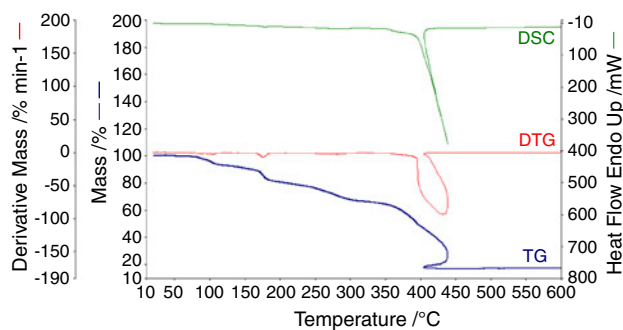


Fig. 3 Thermoanalytical curves of $[\text{Co}(\text{mpk})_2(\text{H}_2\text{O})_2](\text{NO}_3)_2$ (2)

coincides with the gravimetric one (Fig. 2), while the experimental mass loss of 64.40% is much more than theoretical one (52.57%). A possible explanation of this anomalous behavior may be the removal of a small amount of copper(II) complex by the evolved gases of decomposition. The last mpk molecule oxidative decomposition follows as a third step, strong exothermic one (Table 4) temperatures ranging from 160 to 410 °C (24.99% on TG curve). The occurrence of ligand molecule bonded to the metallic center, after the second stage, was confirmed by an additional experiment. The process implies decomposition of initial compound at the same conditions (in air and at 10 K min^{-1}), up to 160 °C, and then spectroscopic IR analysis of the formed residue. IR spectrum (Fig. 7) displays characteristic bands of mpk ligand (1632 cm^{-1} for $\nu(\text{C}=\text{O})$, and 1586 cm^{-1} for $\nu(\text{C}=\text{N})$).

Thermal analysis of $[\text{Co}(\text{mpk})_2(\text{H}_2\text{O})_2](\text{NO}_3)_2$

Figure 3 shows the thermoanalytical curves (TG, DTG, DSC) of $[\text{Co}(\text{mpk})_2(\text{H}_2\text{O})_2](\text{NO}_3)_2$ recorded at 10 K min^{-1} in dynamic air atmosphere using 0.843 mg of sample. As can be seen from these curves, it undergoes a decomposition process with three major steps. First, between 57 and 132 °C the two coordinated water moles are removed from coordination sphere. The experimental mass loss of 7.42% is in good agreement with calculated one of 7.80%. On the second stage, which starts at 132 °C and finishes at 334 °C, 26.60% of the entire cobalt(II) complex is lost. This time, thermal decomposition of two nitrate groups takes place (calculated mass loss 26.89%). The process is accompanied by a weak exothermic effect.

The final step occurs in the temperature range 334–417 °C and represents a succession of two ligand moles eliminations. The strong release of heat which characterizes the transformation ($\Delta H = -12575.1 \text{ J g}^{-1}$) indicates both destruction of all metal-ligand bonds and spontaneous combustion of the organic fragments (experimental weight loss 48.66%, calculated weight loss 52.49%). The mass of the obtained residue corresponds to CoO (found 16.9%,

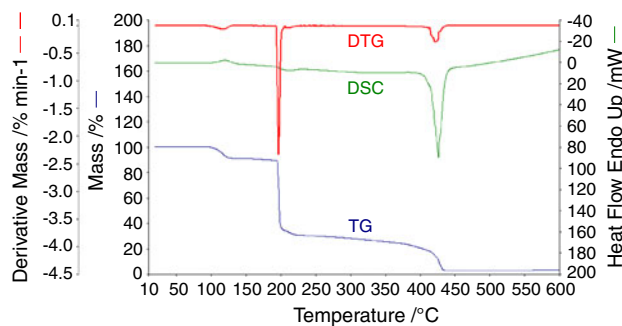


Fig. 4 Thermoanalytical curves of $[\text{Ni}(\text{mpk})_2(\text{H}_2\text{O})_2](\text{NO}_3)_2$ (3)

calculated 16.26%) formation. The violent combustion and spontaneous uncontrollable increase of sample's temperature, forces the TG/DSC Analyzer to stop the temperature program and allow it start again only when the initial temperature is to be reached.

Thermal analysis of $[\text{Ni}(\text{mpk})_2(\text{H}_2\text{O})_2](\text{NO}_3)_2$

In the case of $[\text{Ni}(\text{mpk})_2(\text{H}_2\text{O})_2](\text{NO}_3)_2$ complex, 1.402 mg were used for thermal analysis experiment (Fig. 4). The first step of decomposition is an endothermic process ranging from 90 to 135 °C. Experimental mass loss of about 8.92% may be attributed to the loss of two coordinated water moles (calculated value 7.8%). The next stage, a weak exothermic one (Table 4) occurs between 190 and 230 °C. Due to a spontaneous detachment of two nitrate groups and one ligand mole, an experimental mass loss of 60.85% is registered (sharp profile), which is significantly larger than theoretical one of 53.14%. This phenomenon may be explained through the removal of a small amounts nickel(II) complex, in the same time with the release of heat, just after the chemical reaction.

On the last step, the TG curve of nickel(II) complex shows a mass loss of about 27.55% (250–440 °C) which probable corresponds both to oxidative decomposition of the second ligand mole and to removal of new amounts of nickel derivatives. The stage III is accompanied by a strong exothermic effect with a decrease of the system enthalpy about -4407.2 J g^{-1} (Table 4).

Thermal analysis of $[\text{Zn}(\text{mpk})_2(\text{NO}_3)_2]$

For $[\text{Zn}(\text{mpk})_2(\text{NO}_3)_2]$ a sample of 0.79 mg was heated in the temperature range 20–600 °C at 10 K min^{-1} . The thermoanalytical curves (Fig. 5) exhibit five stages of decomposition, as follows: on first stage (20–60 °C) the mass loss of 3.25% along with a weak endothermic effect indicates a drying of complex (almost constant mass loss rate of 0.01 mg min^{-1} —DTG curve). Between 195 and 273 °C the weight loss is 20.98% which roughly coincides

with the value of 21.35% calculated for the loss of two NO_2 moles from the complex. Insignificantly thermal effect corresponds to this stage. Further decomposition of the previously formed intermediate occurs at 270–435 °C with an endothermic effect of 395.7 J g^{-1} and a loss mass of 29.6% versus 28.07% one meaning the theoretical loss of a single mole of mpk ligand. On the last stage, oxidative decomposition of the second ligand molecule proceeds with a release of heat (Table 4). The mass loss of 35.32% (calculated 31.78%) suggests that this process is accompanied by a removal of a small amount of

decomposition products (4th DTG peak). This is a possible interpretation of the fact that at the end of this stage remains 15.55% zinc(II) oxide as final residue in contrast to the theoretical value of 18.79%.

Thermal analysis of $[\text{Cd}(\text{mpk})_2(\text{NO}_3)_2]$

Thermogravimetric analysis of 0.46 mg $[\text{Cd}(\text{mpk})_2(\text{NO}_3)_2]$ complex (Fig. 6) indicates an oxidative decomposition with three steps: the first one, in the temperature range 80–190 °C, exhibits an experimental mass loss of 10.61%, which may be explained by the loss of one nitrate group (theoretical mass loss $\Delta m_{\text{theor}} = 12.97\%$). This process is not accompanied by a notable thermal effect. The second step takes place between 189 and 410 °C, and involves both the loss of last nitrate group and of one ligand mpk mole. On DSC curve it can be seen a small endothermic effect. The experimental loss of mass ($\Delta m_{\text{exp}} = 37.85\%$) is very close to the theoretical one ($\Delta m_{\text{theor}} = 38.28\%$). The last step, from 410 to 515 °C, represents a strong exothermic oxidative decomposition (Table 4) with an experimental loss of mass of 25.76% versus theoretical one of

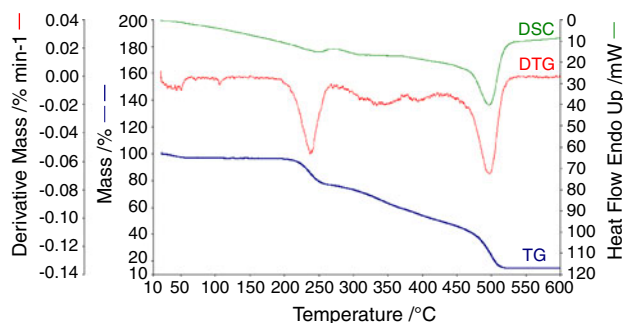


Fig. 5 Thermoanalytical curves of $[\text{Zn}(\text{mpk})_2(\text{NO}_3)_2]$ (4)

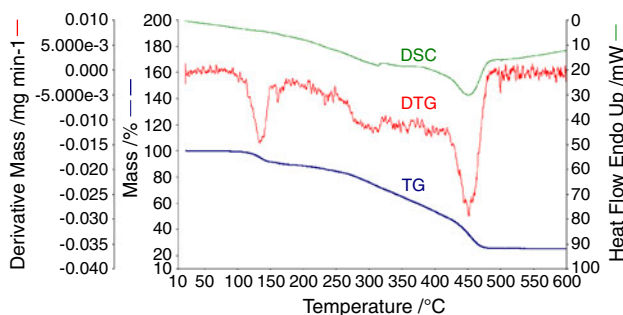


Fig. 6 Thermoanalytical curves of $[\text{Cd}(\text{mpk})_2(\text{NO}_3)_2]$ (5)

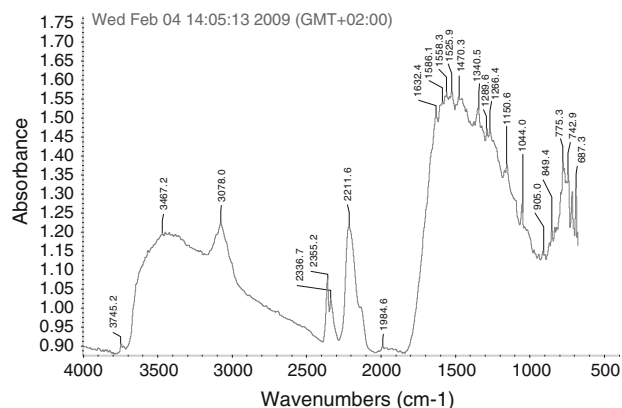


Fig. 7 IR spectrum of $[\text{Cu}(\text{mpk})_2(\text{NO}_3)_2] \cdot 2\text{H}_2\text{O}$ at 160 °C

Table 4 DSC thermal parameters of complexes 1–5 for the heating rate of 10 K min^{-1}

Complex compound	Selected temp. range $T_i - T_f$ (°C)	Thermal effect	Heat flow (mW)	Max. temp. T_{max} (°C)	Transferred heat ΔH (kJ kg^{-1})
$[\text{Cu}(\text{mpk})_2(\text{NO}_3)_2] \cdot 2\text{H}_2\text{O}$	141.5–159.7 (2nd step)	exo	3.2	144.1	−171.7
	275.6–415.5 (3rd step)	exo	31.4	399.4	−5573.0
$[\text{Co}(\text{mpk})_2(\text{H}_2\text{O})_2](\text{NO}_3)_2$	353.7–414.1 (4th step)	exo	360.9	438.6	−12575.1
$[\text{Ni}(\text{mpk})_2(\text{H}_2\text{O})_2](\text{NO}_3)_2$	95.2–138.7 (1st step)	endo	−3.2	120.0	265.4
	193.0–225.1 (2nd step)	exo	2.2	208.7	−171.9
	392.3–447.2 (3rd step)	exo	81.9	426.4	−4407.2
$[\text{Zn}(\text{mpk})_2(\text{NO}_3)_2]$	251.6–307.4 (3rd step)	endo	−1.8	272.9	395.7
	448.1–529.6 (5th step)	exo	24.6	497.4	−5932.9
$[\text{Cd}(\text{mpk})_2(\text{NO}_3)_2]$	368.4–489.5 (3rd step)	exo	13.2	452.0	−7972.6

25.31%. At this stage, the last molecule of mpk is separated from metal center. In fact, this exothermic effect includes two energetic contributions: of the first and the second mole of mpk decomposition. The final product indicates CdO (found: 25.35%; calculated 26.77%).

A final comment about thermal effects which accompanied the last step of decomposition for all complexes is necessary. In all cases, the processes are strong exoenergetic and correspond to oxidative degradation of the second mole of mpk. Only for cobalt(II) complex the thermal effect is double; this behavior is due to simultaneously elimination of the two mpk ligand moles in contrast to others complexes where only one decomposes at this stage (Table 4).

Conclusions

Thermal behavior and spectroscopic investigation of five mpk complexes were carried out. Methyl 2-pyridyl ketone acts as bidentate ligand through N and O atoms, while nitrate groups are monodentate in copper(II) and zinc(II) complexes, bidentate in cadmium(II) complex and ionic in cobalt(II) and nickel(II) compounds according to IR data. The metal ions are six-coordinated, the coordination environment being slightly distorted octahedral, except for the cadmium one which is eight-coordinated. Cd ion is surrounded by two N, O bidentate mpk ligands and two bidentate coordinating nitrate anions, leading to a dodecahedral coordination environment.

Thermal analysis reveals decomposition processes in multiple stages. Data obtained from TG and DTG curves confirm also the presence and the nature of water molecules and the stoichiometry of the studied metal complexes. Generally, water elimination occurs in the first step and the decomposition of nitrate groups and organic ligands in the next stages. The last step of decomposition for all complexes is strong exothermic and corresponds to combustion of the second of mpk mole. In the case of cobalt(II) complex, the thermal effect is double because at this stage both mpk ligands simultaneously decompose.

Acknowledgements The authors are grateful to Mr. Andrei Rotaru for the useful discussions and for the help he provided in writing this paper.

References

1. Highfield JA, Mehta LK, Parrick J, Wardman P. Synthesis, hydroxyl radical production and cytotoxicity of analogues of bleomycin. *Bioorg Med Chem*. 2000;8:1065–73.
2. Dhumwad SD, Gudasi KB, Goudar TR, Goudar CT, Chitnis MP. Synthetic, structural and biological studies of oxovanadium(IV), manganese(II), iron(III), cobalt(II), nickel(II), copper(II) and zinc(II) complexes of 3,4-methylene-dioxymethyl-2-amino-4,5,6,7-tetrahydrobenzothiazole. *Indian J Chem A*. 1995;34:38–42.
3. Das A, Trousdale MD, Ren S, Lien EJ. Inhibition of herpes simplex virus type 1 and adenovirus type 5 by heterocyclic Schiff bases of aminohydroxyguanidine tosylate. *Antiviral Res*. 1999;44:201–8.
4. Klimešová V, Otčenášek M, Waisser K. Potential antifungal agents. Synthesis and activity of 2-alkylthiopyridine-4-carbothioamides. *Eur J Med Chem*. 1996;31:389–95.
5. Kriza A, Tatu M, Stanica N, Anoaica PG. Coordination compounds of several transition metals with phenyl-2-pyridyl-ketone. *Rev Chim Bucharest*. 2008;59:505–10.
6. Tatu M, Kriza A, Maxim C, Stanica N. Synthesis and structural studies of Co(II), Ni(II) and Cd(II) complexes with 2-acetylpyridine. *J Coord Chem*. 2009;62:1067–75.
7. Kriza A, Tatu M, Bolocan-Viasu I, Rogozea AE, Patru E. Synthesis, structural and biological studies of Co(II), Ni(II) and Cu(II) complexes with 2-pyridyl-ketones. *Rev Chim Bucharest*. 2009;60:269–73.
8. Serna ZE, Barandika MG, Cortés R, Urtiaga MK, Barberis GE, Rojo T. Structural analysis and magnetic properties of the dicubane-like tetramer $[\text{Ni}(\text{dpk-OH})(\text{N}_3)]_4 \cdot 2\text{H}_2\text{O}$ (dpk = di-2-pyridyl ketone). *J Chem Soc Dalton Trans*. 2000;29–34.
9. Serna ZE, Lezama L, Urtiaga MK, Arriortua MI, Barandika MG, Cortés R, et al. A dicubane-like tetrameric nickel(II) azido complex. *Angew Chem Int Ed*. 2000;39:344–7.
10. Serna ZE, Cortés R, Urtiaga MK, Barandika MG, Lezama L, Arriortua MI, Rojo T. Investigation of the $\text{Cu}^{\text{II}}/\text{NCS}^-/\text{dpk}$ reaction system in CH_3OH [dpk = di(2-pyridyl) ketone]: isolation, structural analysis and magnetic properties of a dimer and a 1D polymer with the same empirical formula $[\text{Cu}(\text{NCS})_2(\text{dpk-CH}_3\text{OH})]$. *Eur J Inorg Chem* 2001;865–72.
11. Wendlandt WW, Ifitkhar Ali S. The thermal dissociation of some bis and tetrakis(pyridine) metal complexes. *Z Anorg Allg Chem*. 1965;337:6–13.
12. Murgulescu IG, Fatu D, Segal E. Contributions a l'etude cinétique des decomposition endothermiques dans des systemes solide-gaz, a l'aide des donnees thermogravimétriques. *J Therm Anal*. 1969;1:97–106.
13. Mojumdar SC, Simon P, Krutosikova A. [1]Benzofuro[3,2-c]pyridine. Synthesis and coordination reactions. *J Therm Anal Calorim*. 2009;96:103–9.
14. Zhang HY, Zhang JJ, Ren N, Xu NSL, Zhang YH, Tian L, et al. Synthesis, characterization and thermal decomposition kinetics of Sm(III) complex with 2,4-dichlorobenzoate and 2,2-bipyridine. *J Alloys Compd*. 2008;466:281–6.
15. Lalia-Kantouri M, Tzavellas L, Paschalidis D. Novel lanthanide complexes with di-2-pyridyl ketone-p-chloro-benzoylhydrazone. Thermal investigation by simultaneous TG/DTG-DTA and IR spectroscopy. *J Therm Anal Calorim*. 2008;91:937–42.
16. Papatriantafyllopoulou C, Efthymiou CG, Raptopoulou CP, Vicente R, Manessi-Zoupa E, Psycharis V, et al. Initial use of the di-2-pyridyl ketone/sulfate “blend” in 3d-metal cluster chemistry: preparation, X-ray structures and physical studies of zinc(II) and nickel(II) cubanes. *J Mol Struct*. 2007;829:176–88.
17. Olczak-Kobza M. Synthesis and thermal characterization of zinc(II) di(o-aminobenzoate) complexes of imidazole and its methyl derivatives. *Thermochim Acta*. 2004;419:67–71.
18. Skorsepa J, Godocikova E, Cernak EJ. Comparison on thermal decomposition of propionate, benzoate and their chloroderivative salts of Zn(II). *J Therm Anal Calorim*. 2004;75:773–80.
19. Badea M, Olar R, Marinescu D, Segal E, Rotaru A. Thermal stability of some new complexes bearing ligands with polymerizable groups. *J Therm Anal Calorim*. 2007;88:317–21.

20. Badea M, Olar R, Marinescu D, Vasile G. Thermal stability of new complexes bearing both acrylate and aliphatic amine as ligands. *J Therm Anal Calorim.* 2008;92:205–8.
21. Szunyogova E, Mudronova D, Gyoryova K, Nemcova R, Kovarova J, Piknova-Findorakova L. The physicochemical and biological properties of zinc(II) complexes. *J Therm Anal Calorim.* 2007;88:355–61.
22. Diehl KB. Topical antifungal agents: an update. *Am Fam Physician.* 1996;54:1687–92.
23. Tian ZR, Voigt JA, Liu J, McKenzie B, McDermott MJ, Rodriguez MA, et al. Complex and oriented ZnO nanostructures. *Nat Mater.* 2003;2:821–6.
24. Gerstel P, Hoffmann RC, Lipowsky P, Jeurgens LPH, Bill J, Aldinger JF. Mineralization from aqueous solutions of zinc salts directed by amino acids and peptides. *Chem Mater.* 2006;18:179–86.
25. Bauermann LP, Bill J, Aldinger F. Bio-friendly synthesis of ZnO nanoparticles in aqueous solution at near-neutral pH and low temperature. *J Phys Chem B.* 2006;110:5182–5.
26. Kropidłowska A, Rotaru A, Strankowski M, Becker B, Segal E. Heteroleptic cadmium(II) complex, potential precursor for semiconducting CDS layers. *J Therm Anal Calorim.* 2008;91:903–9.
27. Rotaru A, Mietlerek-Kropidłowska A, Constantinescu C, Scarisoreanu N, Dumitru M, Strankowski M, et al. CdS thin films obtained by thermal treatment of cadmium(II) complex precursor deposited by MAPLE technique. *Appl Surf Sci.* 2009;255:6786–9.
28. Nakamoto K. Infrared spectra of inorganic and coordination compounds. New York: Wiley; 1970.
29. Addison CC, Logan N. Anhydrous metal nitrates. *Adv Inorg Chem Radiochim.* 1964;6:71.
30. Lever ABP, Mantovani E, Ramaswamy BS. Infrared combination frequencies in coordination complexes containing nitrate groups in various coordination environments. A probe for the metal nitrate interaction. *Can J Chem.* 1971;49:1957–63.
31. Teyssie P, Charette JJ. Physico-chemical properties of co-ordinating compounds. 3. Infra-red spectra of *N*-salicyclidene-alkylamines and their chelates. *Spectrochim Acta.* 1963;19:1407–23.
32. Lever ABP. Inorganic electronic spectroscopy. Amsterdam: Elsevier; 1984.
33. König E. The nephelauxetic effect. *Struct Bond.* 1971;9:175–212.